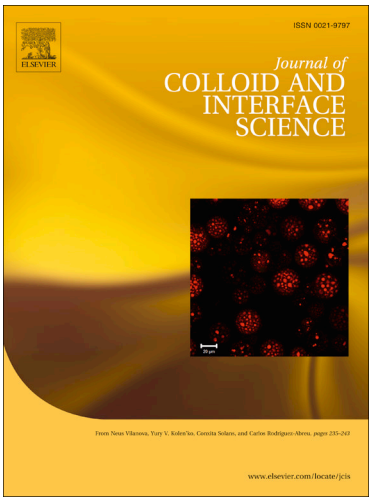

Drugs/lamellae interface influences the inner structure of double-loaded liposomes for inhaled anti-TB therapy: an in-depth small-angle neutron scattering investigation

Eleonora Truzzi, Fiorella Meneghetti, Matteo Mori, Luca Costantino, Valentina Iannuccelli, Eleonora Maretti, Fabio Domenici, Carlo Castellano, Sarah Rogers, Angela Capocefalo, Eliana Leo

PII: S0021-9797(19)30115-8
DOI: https://doi.org/10.1016/j.jcis.2019.01.094
Reference: YJCIS 24583

To appear in: *Journal of Colloid and Interface Science*

Received Date: 18 September 2018
Revised Date: 18 January 2019
Accepted Date: 22 January 2019

Please cite this article as: E. Truzzi, F. Meneghetti, M. Mori, L. Costantino, V. Iannuccelli, E. Maretti, F. Domenici, C. Castellano, S. Rogers, A. Capocefalo, E. Leo, Drugs/lamellae interface influences the inner structure of double-loaded liposomes for inhaled anti-TB therapy: an in-depth small-angle neutron scattering investigation, *Journal of Colloid and Interface Science* (2019), doi: https://doi.org/10.1016/j.jcis.2019.01.094

Drugs/lamellae interface influences the inner structure of double-loaded liposomes for inhaled anti-TB therapy: an in-depth small-angle neutron scattering investigation

Eleonora Truzzi,[a,‡] *Fiorella Meneghetti,*[b,‡] *Matteo Mori,*[b] *Luca Costantino,*[a] *Valentina Iannuccelli,*[a] *Eleonora Maretti,*[a] *Fabio Domenici,*[c,*] *Carlo Castellano,*[d,*] *Sarah Rogers,*[e] *Angela Capocefalo,*[f] *Eliana Leo*[b,*]

[a] Dipartimento Scienze della Vita, *Università degli Studi di Modena e Reggio Emilia*, via Campi 103, 41121 Modena Italy;

[b] Dipartimento di Scienze Farmaceutiche, *Università degli Studi di Milano* Via L. Mangiagalli 25, 20133 Milano, Italy;

[c] Dipartimento di Scienze e Tecnologie Chimiche, Via della Ricerca Scientifica, *Università degli Studi di Roma Tor Vergata* 00133 Roma Italy;

[d] Dipartimento di Chimica, *Università degli Studi di Milano* via Golgi 19, 20133 Milano, Italy;

[e] ISIS-STFC, Rutherford Appleton Laboratory, Harwell Oxford, Didcot OX11 0QX, UK;

[f] Dipartimento di Fisica, *Sapienza Università di Roma* P. le Aldo Moro 5, 00185 Roma, Italy.

Author Information

Corresponding Authors

*eliana.leo@unimore.it , Tel. +39 059 205 8558, ORCID: 0000-0003-4721-1676.

*carlo.castellano@unimi.it , Tel. +39 0250314449, Fax +39 0250314454, ORCID: 0000-0002-7497-0670

*fabio.domenici@uniroma2.it , Tel. +39 0672594464, Fax +39 0672594328, ORCID: 0000-0001-6776-2737

Author Contributions.

‡These authors contributed equally.

Abstract

With the aim of developing new drug carriers for inhalation therapy, we report here an in depth investigation of the structure of multilamellar liposomes loaded with two well-established anti-tubercular (anti-TB) drugs, isoniazid (INH) and rifampicin (RIF), by means of small-angle neutron-scattering (SANS) analysis. Unloaded, single drug-loaded and co-loaded liposomes were prepared using different amounts of drugs and characterized regarding size, encapsulation efficiency and drug release. Detailed information on relevant properties of the investigated host-guest structures, namely the steric bilayer thickness, particle dispersion, number of lamellae and drug localization was studied by SANS. Results showed that RIF-liposomes were less ordered than unloaded liposomes. INH induced a change in the inter-bilayer periodical spacing, while RIF-INH co-loading stabilized the multilamellar liposome architecture, as confirmed by the increment of the drug loading capacity. These findings could be useful for the understanding of *in vitro* and *in vivo* behavior of these systems and for the design of new drug carriers, intended for inhaled therapy.

KEYWORDS: multilamellar liposomes; drugs-lamellae interactions; small-angle neutron scattering; isoniazid; rifampicin.

1. Introduction

Tuberculosis (TB) is one of the world's deadliest communicable diseases [1]. Since *Mycobacterium tuberculosis* (Mtb) tends to localize in the lungs, the administration of therapeutic agents through the pulmonary route could be a valid strategy to improve the efficacy of drugs, as it allows the deposition of the active pharmaceutical ingredient (API) directly at the infection site, avoiding first-pass metabolism and reducing systemic side effects. Recently, liposomes have been proposed as new drug delivery carriers for inhalation therapy, to improve drug targeting and delivery [2,3]. The success of targeting alveolar macrophages depends critically on the chemico-physical characteristics of the nanocarriers, namely their size, shape, density, porosity, surface charge and presence of specific molecules involved in the receptor-mediated endocytosis [2,4]. Rifampicin (RIF) and isoniazid (INH), two powerful first-line anti-TB drugs provided with a very different water solubility (INH LogP -0.64 and RIF LogP 3.719) [5,6], were here chosen as drug models for co-loading experiments, using conventional liposomes prepared with phosphatidylcholine (PC) and cholesterol (Chol). Considering the liposomal architecture, both the hydrophilic INH and the hydrophobic RIF were encapsulated within the nanoparticle, as they could interact with its different components, namely the lipid bilayers (RIF) and the central aqueous core (INH) [7]. Therefore, it was conceivable that these drugs could be located inside the liposomal formulations, as depicted in the model shown in Figure 1.

Taking into account that the co-administration of RIF and INH (Rifinah®) improves the outcomes in TB patients, we co-loaded these two drugs in the same formulation for pulmonary delivery. Following this approach, these nanocarriers may acquire better pharmacokinetic properties, thus ensuring greater efficacy [8]. This strategy could also be conveniently applied for the administration of non-traditional antitubercular agents, targeting new druggable molecular pathways [9–11], with the aim of tackling the growing incidence of drug resistant infections [12]. In addition, the formulation of carriers, shipping high amounts of drugs, generally improves patient compliance and reduces systemic adverse effects.

In order to fully address these issues, an in-depth characterization of the nanocarriers is of critical importance for optimizing the loading conditions. Among the available techniques, small-angle neutron scattering (SANS) has recently emerged as a powerful tool to investigate amphiphilic aggregates, such as uni-lamellar and multi-lamellar vesicles [13]. In particular, SANS provides crucial information about the arrangement and behavior of the drug into the nanoparticle after its encapsulation and allows the analysis of these systems at nanometric level. This technique yields valuable and unique data about steric bilayer thickness, particle dispersion and the finer structural features. In detail, it is possible to determine: the core radius (r_c), the shell thickness (t_s), the shell scattering length density (SLD, ρs), the water layer thickness (t_w), the water scattering length density (SLD, $\rho 0$), the number of layers (N) and the overall liposome size (see Figure 2) [14].

Therefore, we decided to apply this technique on liposomes co-loaded with RIF and INH, comparing this formulation with mono-loaded liposomes, in order to deeply characterize the structure of the carrier and any perturbation induced by the presence of these drugs, under physiological conditions and without any earlier manipulation [15]. We complemented this SANS study with Photon Correlation Spectroscopy (PCS) analysis and drug release studies, in order to obtain key information on our new host-guest structures, for a synergistic and site-specific antitubercular therapy.

2. Materials and Methods

2.1 Materials

Cholesterol (Chol, ≥99%) was purchased from Sigma Aldrich (St. Luis, MO, USA), phosphatidylcholine (PC, 95%) from Egg yolk was obtained by Fluka Chemie (Buchs, Switzerland). Rifampicin (RIF, Lot. No 17447/BR, purity calculated according current Ph. Eur.: 97-102%) was a kind gift from Sanofi (Brindisi, Italy), while Isoniazid (Isonicotinic Acid Hydrazide, INH, 98.0%) was purchased from T.C.I Europe (Zwijndrecht, Belgium). Finally, deuterium oxide (D_2O, Lot. 170009, 99.96%) was purchased from VWR (Milan, Italy). All solvents employed were of analytical grade.

2.2 Liposome preparation

Liposomes were prepared using the Reverse Phase Evaporation (REV) technique and homogenized using an Ultraturrax device (Ika-euroturrax T 25 basic, IkaLabortechnik, Staufen, Germany) [16].

Cholesterol (Chol) and phosphatidylcholine (PC) with fixed molar ratio (1:1) were weighed and solubilized in chloroform at the final concentration of 40 mM. The obtained solution was placed into a glass flask, and the solvent was removed under vacuum at room temperature until the formation of a dry film (Buchi HB-140, Buchi, Swiss). The phospholipid film was re-dissolved in diethyl ether and mixed with water (3:1 ratio). This suspension was vortexed to form a W/O emulsion; than the emulsion was stirred for 2 hours at 200 rpm to remove the organic solvent, inducing the phase reversal and, finally, the formation of liposomes (MLV). Liposomes were homogenized by Ultraturrax (Ika-euroturrax T 25 basic, IkaLabortechnik, Staufen, Germany) for 3 minutes and purified by dialysis for 30 minutes in order to separate the free drugs before being stored at +4 °C in vials. For loaded liposomes, RIF:lipid (w/w) ratios of 3:100, 6:100, 12:100 (for RIF 3%, 6%, 12% samples, respectively) were used, adding the drug to the chloroform solution along with the lipids; for INH-loaded liposomes 15:100, 30:100, 60:100 drug:lipid (w/w) ratios were employed (for INH 15%, 30%, 60% samples, respectively), adding INH to the water phase mixed with diethyl ether. For the preparation of liposomes encapsulating INH and RIF (Co-loaded liposomes), a RIF:INH:lipid (w/w) ratio of 12:15:100 was employed.

For SANS analysis, liposomes were prepared and purified using D_2O instead of milliQ water.

2.3 Photon Correlation Spectroscopy (PCS)

Liposome size and polydispersity index (PDI) were determined by photon correlation spectroscopy (PCS) technique using a Zetasizer Nano ZS analyzer system (Zetasizer version 6.12; Malvern Instruments, Worcs, U.K.). The results were expressed as the average of three different measurements.

Analysis was performed in triplicate and each measurement was averaged over at least 12 runs.

2.4 Drug loading and Encapsulation Efficiency

The drug loading (DL %) and the encapsulation efficiency (EE %) of loaded-liposomes were evaluated by UV-visible spectroscopy (Lambda 3B Perkin-Elmer, Wotham, USA). For the determination of the hydrophilic drug (INH), 300 µL of liposomal suspension was dissolved in 1.5 mL of isopropanol and this solution was diluted with MilliQ water. The amount of incorporated INH was determined in the solution by recording the absorbance at λ = 262 nm. In the same way, for the determination of RIF, 300 µL of liposomal suspension was dissolved in 1.5 mL of isopropanol and this solution was diluted with methanol. The amount of incorporated RIF was determined by recording the absorbance at λ = 475 nm.

The absorbance of the solutions containing the drugs was converted to the amount of drug by preparing standard calibration curves constructed using supernatants of the corresponding unloaded liposomes (n = 6), in order to eliminate any possible interference in the measurements.

The direct quantification of drug amounts in co-loaded liposomes using UV-visible spectroscopy cannot be performed, since INH absorption spectrum is overlapped to that of RIF [17]. For this reason, to determine INH peak-to-peak first-order derivative, UV spectroscopy was employed. Gürsoy *et al*. demonstrated the reliability of derivative UV spectrophotometry for the simultaneous estimation of RIF and INH, avoiding the interference problem related to spectral overlap at 262 nm [18].

DL % and EE % were calculated with the following equations:

$$DL\,\% = \frac{incorporated\ drug\ (mg)}{total\ mass\ of\ liposomes\ (lipids\ and\ drug)} * 100$$

$$EE\,\% = \frac{incorporated\ drug\ (mg)}{amount\ of\ drug\ added\ (mg)} * 100$$

The method to determine the amount of RIF and INH in liposomes has been validated by using unloaded liposomes spiked with known quantities of drugs.

2.5 Drug release studies

The *in vitro* release of RIF and INH from liposomes was analyzed in Simulated Lung Fluid (SLF) at pH 7.4 [19]. Briefly, 1 mL of liposome suspension placed in a semipermeable membrane (Dialysis Tubing - Visking MWCO-12-14000 Daltons, Medicell International Ltd, London) was immersed into a vessel containing 30 mL of SLF medium and maintained at 37 ± 0.5 °C under gentle stirring. At fixed time intervals, aliquots (1 ml) were withdrawn from the solution and INH and/or RIF content was determined by spectrophotometry, as previously described (Lambda 35). Two aliquots were analyzed for each time point using unloaded liposomes as blank and the study was performed in triplicate.

2.6 SANS experiment

Nanoparticles characterization was undertaken using the fixed-geometry, time-of-flight small angle neutron scattering Sans2d instrument at the ISIS Spallation source at the Rutherford Appleton Laboratory, U.K.

A scattering vector $q = (4\pi/\lambda) \sin(\theta)$ (where λ is the neutron wavelength and 2θ is the scattering angle) range between 0.001 and 0.5 $Å^{-1}$ was obtained by using neutron wavelengths spanning from 2.2 to 10 Å, with a sample–detector distance of 4 and 12 m.

The samples were contained in 2 mm path length, UV-spectrophotometer grade, quartz cuvettes and mounted on aluminum holders on top of an enclosed, computer-controlled, sample chamber. Temperature control was achieved by using a thermostated circulating bath pumping fluid through the base of the sample chamber, achieving a temperature stability of ± 0.2 °C. The experiments were run at 25 °C using 0.6 mL volume samples in quartz cuvettes (Hellma, GmbH). To maintain the degree of purity of D_2O and avoid phenomena of deuterium chemical exchange, the SANS measurements were performed in controlled hermetic conditions.

All scattering data were (a) normalized for the sample transmission, (b) background corrected using a quartz cell filled with the solvent used (D_2O), and (c) corrected for the linearity and efficiency of the detector response (component of the instrumental smearing) using the instrument specific software package [20]. The experimental time of a single measurement was between 30 and 60 minutes.

The experimental data were analyzed using the multi-shell spherical model of the fitting routine SASView 2.2.0, in the context of a spherical core-shell morphology.

SANS experiments were carried out to quantify the specific type of aggregated system (observed by the previous techniques), in terms of shape and size characteristics. The scattering intensity detected by this

technique contains intra-particle information (size, shape) and inter-particle information (interactions between the scattering centers of the aggregated systems) in solution (eqn (1)),

$$I(q) = N_p V_p^2 \Delta\rho^2 P(q) S(q) + B \qquad (1)$$

where N_p is the number of scattering particles per unit volume, V_p is the volume of one scattering particle, $\Delta\rho$ is the difference in scattering length density (SLD) in the system (known as contrast), P(q) is the form factor and gives intra-particle information (size and shape), S(q) is the structure factor and gives inter-particle information (particle interactions), B is the background signal.

According to the employed model [21], the scattering intensity of non-interacting (S(q) ~ 1) multilamellar vesicles is given by the formula:

$$I(q) = \frac{\Phi}{V(R_N)}(\rho_S - \rho_0)^2 \left[\sum_{i=1}^{N} 3V(r_i)\frac{\sin(qr_i) - qr_i\cos(qr_i))}{(qr_i)^3} - 3V(R_i)\frac{\sin(qR_i) - qR_i\cos(qR_i))}{(qR_i)^3}\right]^2 \qquad (2)$$

where Φ is the volume fraction of the particles in solution, R_N is the total radius of the multilamellar liposome containing N layers, $V(r)$ is the volume of a sphere with radius r, ρ_S is the shell SLD, ρ_0 is the solvent SLD, , $r_i = r_c + (i-1)(t_s + t_w)$ with r_c water core radius and t_s and t_w thickness of the lipid layer and of the solvent, respectively; $R_i = r_i + t_s$. The size $2R_N$ of the multilamellar vesicles is calculated from the values of the parameters extrapolated from the best fits of the SANS curves according to the formula $2R_N = 2r_C + N \cdot 2t_s + (N-1) \cdot 2t_w$.

In the fitting procedure and data analysis, the following foresights have been employed: (a) a polydispersity (PDI) following a Gaussian distribution has been considered for the structural parameters r_c, t_s and t_w; (b) the SLD values ρ0 and ρs (with default scale was 1 and background 0.02 cm^{-1}) were initialized according to literature [22] and optimized in the fitting procedure in order to evaluate SLD changes attributable to the presence of the drugs, both in the water and in the lipid layers; (c) the fit quality was determined by the reduced χ^2 value, which is reported in the caption of the corresponding Figures. Neither aggregation processes nor appearance of precipitate were revealed by visual inpection. In this respect, the SANS measurement was repeated twice to ensure that the system was effectively at equilibrium.

Due to the huge difference in the coherent scattering lengths of deuterium and hydrogen, the D_2O/H_2O contrast variation SANS methodology allows a well distinguished scattering from the shell with respect to the corresponding inner content. Therefore, by using D_2O in the external phase of the liposomal system, we gained information on the morphology and structure of the lipid shell correlated to the loaded drug placement.

2.7 Statistical analysis

Statistical analysis was performed using the one-way analysis of variance (ANOVA). The data are represented as means ± SD. Differences were considered statistically significant at p-values less than 0.05 (*$p<0.05$; **$p<0.01$; ***$p<0.005$).

3. Results

3.1 Liposome characterization

Data of size, polydispersity index (PDI), determined by PCS analysis, encapsulation efficiency and drug loading of the analysed liposomes are shown in Table 1.

No significant size differences could be appreciated between the drug-loaded liposomes and the unloaded samples. With respect to particle size distribution, the polydispersity index (PDI), used to define the degree of homogeneity of a size distribution of particles, is a parameter given by the Zeta sizer analyzer System. Generally, a PDI of 0.3 and below is considered to be acceptable for drug delivery systems and indicates a monomodal distribution of vesicles [23]. Regarding this value, we observed that if we increased the amount of RIF from 3 mg to 12 mg, a PDI increment from 0.283 to 0.440 followed. With respect to INH-loaded liposomes, differences neither in size nor in PDI values could be appreciated in the differently concentrated drug-loaded samples. Finally, the co-loaded sample presented the same size and intermediate PDI value as compared to the homologous single loaded samples.

Concerning encapsulation efficiency, UV-vis spectroscopy analysis indicated that about 50% of both the drugs were incorporated in each sample, regardless of the drug/lipid ratio adopted. As for the drug loading capacity, this parameter increased proportionally with the initial amount of added drug. The co-loading of RIF and INH in the liposomes significantly increased the encapsulation efficiency, with respect to the formulations containing the equivalent amount of the single drug.

3.2 Release studies

As shown in Figure 3, single loaded RIF and INH liposomes showed no significant differences in the drug release profile, independently to the amount of drug loaded. In agreement with its hydrophilic features, INH release rate was faster than that of RIF: 80-90% of INH was released in 5 hours, whereas 25-35% of RIF was released in the same time frame. As for the co-loaded liposomes, each drug showed the same release rate of the homologous single-loaded liposomes.

3.3 SANS experiment

The SANS data are displayed in Figures 4-6, as absolute scattering intensity (shifted vertically) plotted as a function of the scattering vector q. Error bars correspond to one standard deviation of the mean scattering intensity. Figures 4-6 reports the superimposed SANS profiles of representative samples of liposomes loaded with different concentrations of RIF, INH and both drugs respectively, together with the corresponding best fit performed by SasView by using the well-established multi-lamellar vesicle model [19]. This model provides the form factor, P(q), for a multi-lamellar vesicle depicted in Figure 2 with N lipid-drug shells of a span t_s and a scattering length density ρ_s, where the core is filled with solvent and the

shells are interleaved with solvent-drug layers of a span t_w and a scattering length density ρ_0. All the parameters extrapolated from the best fits are reported in Tables 2 and 3.

Unloaded liposomes assemble in solution as oligo-lamellar vesicles constituted of roughly 6 concentric bilayers giving rise to a periodicity of ~ 68 Å (shell + water thickness), compatible with the thickness of each bilayer [24]. The vesicles are stable and show a spherical shape, well-matched with the best fit model used, with a size of ~ 420 nm (Table 2).

Regarding RIF-loaded liposomes, a reduction in the shell scattering length density (SLD, ρ_s) with respect to the unloaded liposomes was observed. This effect is symptomatic of structural modifications of the lipid bilayers due to a different packing of the lipid molecules upon the inclusion of the hydrophobic drug. On the contrary, no significant perturbations were appreciated in SLD of deuterated water confined among the shells and in the core of liposomes.

Such RIF hydrophobic interaction modifies the structure of the multi-lamellar arrangement, in proportion to the concentration of the drug in the lipid (from 3% to 12%) (Figure 4). In particular, starting from RIF at 6% concentration, we detected a reduction of the lamellae number with a concomitant slight increase in the periodical spacing, given by the repetition of the liposome lipid bilayers, and polydispersity of the shell thickness, obtained comparing the best fit parameter values, which changes to 0.5 and 0.6 for RIF at 6% and 12% respectively, compared to 0.3 obtained for the lowest RIF concentration. In addition, no significant aggregation was detected. The best fit results are reported in Table 2.

Regarding INH-loaded liposomes, the hydrophilic drug does not seem to induce significant changes in the multi-lamellar assembly of unloaded liposomes (Figure 5). In fact, our results indicate that the lamellae number of oligo-lamellar vesicles is maintained up to 60% of INH (Table 2). At the highest tested concentration, the drug embedded within the liposomes induced a slight but significant decrease in the water-drug phase SLD, ρ_0 of the system, with a change in the inter-bilayer periodical spacing and a slight change in size of the liposomes.

Finally, the effect of the co-loading of both drugs on the liposomes was examined. Taking into account the structural modification which can affect the liposome stability due to the presence of the drugs, the combination of RIF at 12% and INH at 15% was chosen. In co-loaded liposomes the structure of the multi-lamellar arrangement was not affected by the presence of RIF. This is in contrast with the results obtained for RIF-loaded liposomes, despite the same amount of RIF was used in the formulation. The SANS data depicted in Table 3 indicated the presence of the drugs both in the water compartments and in the bilayer. Moreover, the vesicle demonstrated to be stable with a spherical shape, as evidenced from the goodness of the best fit with a multi-shell spherical model.

In order to better visualize the obtained results, the SLD profiles have been reconstructed from the values of the structural parameters, extrapolated from the best fits, as a function of the liposome radius. The profiles obtained for the liposomes loaded with the highest drug concentrations (RIF 12% and INH 60%) and

liposomes co-loaded with both the drugs (RIF 12% and INH 15%) are reported in Figure S1, in comparison with the unloaded sample.

4. Discussion

Liposomes here described, co-incorporating RIF and INH, are intended for inhaled chemotherapy against pulmonary TB; they were designed to reach a higher antimycobacterial potency and improve the drug therapeutic profile [25]. The addition of two different drugs inside liposomal vesicles could alter the carrier structure; therefore, we performed an in-depth structural study in order to investigate any possible destabilization of the liposome framework.

PCS analyses on the liposome samples showed no differences in size, regardless of the type and amount of the embedded drug. All the samples have an average diameter around 350 nm, demonstrating the suitability to be analyzed by SANS (Table 1) [14]. Regarding the PDI value, we observed some differences among the analyzed samples. For RIF-loaded liposomes, a parallel increase in the PDI values with the drug loading was detected, suggesting a drop of size homogeneity when an increase of drug loading occurred. This effect might be due to changes in the structural organization of the lipid bilayer caused by the hydrophobic drug, which may interact with phospholipid tails of the liposome lamellae [26,27]. In INH-loaded liposomes, the size homogeneity did not change with the increase of the drug loading, probably because INH is highly soluble in water and its interaction with the phospholipid lamellae is low. Finally, PCS analysis of co-loaded liposomes showed an intermediate value of PDI, with respect to the loaded and unloaded samples, indicating the opposite influence of the two drugs on the homogeneity of the vesicle size.

The results of PCS analysis were further supported by SANS data. By fitting the scattering curves, a destabilization of liposomal structure of RIF-loaded liposomes was highlighted. The fit parameters showed that the size underwent a slight decrease (too small to be detected by PCS analysis) with respect to the unloaded carrier. This modification is probably due to interactions between the hydrophobic tails of phospholipids and RIF. Moreover, at higher concentrations, the Bragg peak, indicating the spacing of the planes satisfying the Bragg's law, was wider and the lamellar structure appeared destabilized. The behavior in the presence of the hydrophilic drug INH was different, since liposome dimension and multi-lamellar assembly did not significantly change up to 60% of INH. The hydrophilicity of this drug leads to its confinement in the aqueous environment of the core and in the inter-bilayer spaces composing the liposome shell. Relevant changes in the stereochemistry of the multilamellar vesicles and, in particular, in the thickness of the water and lipid layers t_w and t_s are not observed at the lower INH concentrations (15% and 30%). In contrast, for the sample with the highest INH concentration, a slight but significant decrease in both ts and tw is detectable, along with a decrease in the number of lamellae and a lower measured size (~ 403 nm). The position of INH within the liposome is also confirmed by water-drug layer SLD ρ_0, whose value decreases with the drug concentration respect to that of pure D_2O. Moreover, the change in the inter-

bilayer periodical spacing suggests the formation of interactions between the drug and the phospholipid heads, at the water-lipid interface. These interactions are probably hydrogen bonds or van der Waals forces, giving rise to slight changes in the liposome size, which cannot be detected by PCS analysis. In more detail, the interaction of the phosphate region of the phosphatidylcholine's polar heads with the INH molecules could enhance the choline motional freedom [28], affecting the packing of the lipid bilayer. This effect is coherent with the observed decrease of the lipid bilayer thickness, which shifts from 5.0 nm for the unloaded samples to 4.8/4.6 nm for the INH-loaded vesicles. Notably, the disorganization of the lipids within the bilayer leads to an increment of the membrane fluidity, promoting the penetration of water molecules [29] and thus resulting in a slight increase of the shell SLD ρs for all the INH-loaded samples with respect to that of the control.

As confirmed by PCS studies, the SANS profiles for the co-loaded liposomes highlighted that, in the experimental condition adopted, it is possible to obtain stable liposomes co-embedded with both drugs. Notably, SANS data suggested that the hydrophobic RIF determines a large destabilization of the multi-lamellar vesicular structure, while the co-presence of INH and RIF causes an intriguing stabilization effect on the oligo-lamellar shelled liposome (Table 3). This synergistic effect promoted the uptake of both drugs inside the vesicles, as confirmed by the drug loading results. Taking into account the previous outcomes, it is important to underline that co-loaded liposomes proved to be able to incorporate higher amount of both drugs, even if the loading capacity was high for INH but not for RIF. This effect was previously observed in other studies and it was attributed to the enhanced solubility of RIF and INH in mixture [18]. On the basis of the results of SANS analysis, it is possible to provide a more detailed description for this phenomenon. The increased amount of RIF loaded might be explained by the structure stabilization exerted by the co-presence of INH, while the higher INH loading could be attributable to an increase in the lipid bilayer rigidity, induced by the intercalation of the hydrophobic RIF, during liposome formation. To the best of our knowledge, SANS data corroborate information provided by other spectroscopic techniques reported in the literature [26,27].

With regard to drug release, this effect did not elicit any significant variation in the *in vitro* behavior of these systems. Despite the different localization of the two drugs within the nanocarriers, the presence of RIF and IHN in the same liposome did not modify the release profiles of each drug, which remained substantially unaltered with respect to those of the mono-loaded formulations. A similar result was obtained by Gürsoy *et al.* [18], who used liposomes constituted of natural phosphatidylcholine, which possessed a low transition temperature, resulting in high membrane fluidity [30].

Conclusions

In this paper, we studied several liposome formulations as carriers for the most used anti TB-drugs: RIF and INH. Our data demonstrated the importance of SANS in defining not only the drug localization (expected data), but also the role that the drugs play in contributing to the stability of single and co-loaded liposomes. Studies performed with liposomal forms of tuberculostatics showed that the bilayer composition is critical for targeting liposomes and for obtaining stable drug-liposome formulations [31]. Moreover, a comprehensive study explaining the complex interaction between these drugs and liposomes is still lacking.

We showed that the SANS technique is able to define RIF and INH localization within MLV liposomes and drug-lipids interactions, providing important clues for obtaining stable nanoparticles to be used in tuberculosis therapy. In particular, we calculated the size of MLV and we obtained detailed information on their fine structure. Moreover, we described the changes, both in the water and in the lipid layers, attributable to the presence of the drugs, as these latter interfered with the MLV self-assembling. In the case of RIF-loaded liposomes, the hydrophobic molecules, embedded in the lipid bilayers, altered the lipid organization in the lamellae; we highlighted that this effect depends on the RIF concentration. Regarding the interaction of the hydrophilic INH with the phospholipid heads at the water-lipid interfaces, we evidenced that INH affected the bilayer structure as well as the organization of the coordinated water, in the water leaflet between the lamellae. The penetration of water molecules in the bilayer increased the distances between lipid molecules, producing in this way a sort of "membrane fluidification effect". When RIF and INH are co-loaded, the SANS data demonstrated that a sort of stabilization of the structure and dimension of the liposome occurred, which might promote, in a synergistic way, the embedding of both drugs.

In conclusion, SANS analysis supplies much more detail about the size than PCS and provides in depth information about the architecture of liposomes, allowing to better understand the effects and the localization of these drugs inside the liposomes. In addition, the stabilization effect on the structure and dimensions of the liposome when RIF and INH are co-administered is an encouraging result for the development of more efficient nanoparticles.

All these outcomes represent the key preliminary step for the understanding of the *in vitro* and *in vivo* behavior of these systems and for the designing of new drug carriers, intended for inhalation therapy.

Notes

The authors declare no competing financial interest.

Acknowledgments

This work was funded by University of Milan (Linea B) and by University of Modena and Reggio Emilia (DSV-FAR 2015).

References.

[1] World Health Organization, Global Tuberculosis Report 2017, Geneva, 2017.

[2] S. Claus, C. Weiler, J. Schiewe, W. Friess, How can we bring high drug doses to the lung?, Eur. J. Pharm. Biopharm. 86 (2014) 1–6. doi:10.1016/j.ejpb.2013.11.005.

[3] L.-O. Larsson, New approaches in drug treatment for tuberculosis: Inhalation using liposomes only a future vision or soon in clinical practice?, Int. J. Mycobacteriology. 5 (2016) S29–S30. doi:10.1016/j.ijmyco.2016.09.032.

[4] V. Iannuccelli, E. Maretti, Inhaled Micro-or Nanoparticles: Which are the Best for Intramacrophagic Antiinfectious Therapies? Intramacrophagic Anti-infectious therapies, J Infect Dis Diagn. (2015). doi:10.4172/2576-389X.1000e102.

[5] P.J. Brennan, D.B. Young, Isoniazid, Tuberculosis. 88 (2008) 112–116. doi:10.1016/S1472-9792(08)70011-8.

[6] P.J. Brennan, D.B. Young, Rifampicin, Tuberculosis. 88 (2008) 151–154. doi:10.1016/S1472-9792(08)70024-6.

[7] C. Grabielle-Madelmont, S. Lesieur, M. Ollivon, Characterization of loaded liposomes by size exclusion chromatography, J. Biochem. Biophys. Methods. 56 (2003) 189–217. doi:10.1016/S0165-022X(03)00059-9.

[8] J. Costa-Gouveia, E. Pancani, S. Jouny, A. Machelart, V. Delorme, G. Salzano, R. Iantomasi, C. Piveteau, C.J. Queval, O.-R. Song, M. Flipo, B. Deprez, J.-P. Saint-André, J. Hureaux, L. Majlessi, N. Willand, A. Baulard, P. Brodin, R. Gref, Combination therapy for tuberculosis treatment: pulmonary administration of ethionamide and booster co-loaded nanoparticles, Sci. Rep. 7 (2017) 5390. doi:10.1038/s41598-017-05453-3.

[9] L. Fanzani, F. Porta, F. Meneghetti, S. Villa, A. Gelain, A.P. Lucarelli, E. Parisini, Mycobacterium tuberculosis Low Molecular Weight Phosphatases (MPtpA and MPtpB): From Biological Insight to Inhibitors., Curr. Med. Chem. 22 (2015) 3110–32. doi:10.2174/0929867322666150812150036.

[10] F. Meneghetti, S. Villa, A. Gelain, D. Barlocco, L.R. Chiarelli, M.R. Pasca, L. Costantino, Iron

Acquisition Pathways as Targets for Antitubercular Drugs., Curr. Med. Chem. 23 (2016) 4009–4026. doi:10.2174/0929867323666160607223747.

[11] V. Singh, V. Mizrahi, Identification and validation of novel drug targets in Mycobacterium tuberculosis, Drug Discov. Today. 22 (2017) 503–509. doi:10.1016/J.DRUDIS.2016.09.010.

[12] L. D'Ambrosio, R. Centis, S. Tiberi, M. Tadolini, M. Dalcolmo, A. Rendon, S. Esposito, G.B. Migliori, Delamanid and bedaquiline to treat multidrug-resistant and extensively drug-resistant tuberculosis in children: a systematic review., J. Thorac. Dis. 9 (2017) 2093–2101. doi:10.21037/jtd.2017.06.16.

[13] N. Kučerka, M.-P. Nieh, J. Pencer, T. Harroun, J. Katsaras, The study of liposomes, lamellae and membranes using neutrons and X-rays, Curr. Opin. Colloid Interface Sci. 12 (2007) 17–22. doi:10.1016/J.COCIS.2006.11.006.

[14] N. Kučerka, J.F. Nagle, J.N. Sachs, S.E. Feller, J. Pencer, A. Jackson, J. Katsaras, Lipid Bilayer Structure Determined by the Simultaneous Analysis of Neutron and X-Ray Scattering Data, Biophys. J. 95 (2008) 2356–2367. doi:10.1529/biophysj.108.132662.

[15] E. Di Cola, I. Grillo, S. Ristori, Small Angle X-ray and Neutron Scattering: Powerful Tools for Studying the Structure of Drug-Loaded Liposomes., Pharmaceutics. 8 (2016) 10. doi:10.3390/pharmaceutics8020010.

[16] F. Sacchetti, D. D'Arca, F. Genovese, S. Pacifico, E. Maretti, M. Hanuskova, V. Iannuccelli, M.P. Costi, E. Leo, Conveying a newly designed hydrophilic anti-human thymidylate synthase peptide to *cisplatin* resistant cancer cells: are pH-sensitive liposomes more effective than conventional ones?, Drug Dev. Ind. Pharm. 43 (2017) 465–473. doi:10.1080/03639045.2016.1262870.

[17] M. Tilinca, G. Hancu, E. Mircia, D. Iriminescu, A. Rusu, R.A. Vlad, E. Barabás, Simultaneous determination of isoniazid and rifampicin by UV spectrophotometry, Farmacia. 65 (2017) 219–224.

[18] A. Gürsoy, E. Kut, S. Özkirimli, Co-encapsulation of isoniazid and rifampicin in liposomes and characterization of liposomes by derivative spectroscopy, Int. J. Pharm. 271 (2004) 115–123. doi:10.1016/j.ijpharm.2003.10.033.

[19] M.R.C. Marques, R. Loebenberg, M. Almukainzi, Simulated Biological Fluids with Possible Application in Dissolution Testing, Dissolution Technol. 18 (2011) 15–28. doi:10.14227/DT180311P15.

[20] V. Ramakrishnan, A Treatment of Instrumental Smearing Effects in Circularly Symmetric Small-Angle Scattering, J. Appl. Cryst. 18 (1985) 42–46. doi:10.1107/S0021889885009748.

[21] B. Cabane, Small Angle Scattering Methods, in: M.D. R. Zana (Ed.), Surfactant Solut. New Methods Investig., Surfactant, 1987.

[22] F. Domenici, C. Castellano, A. Congiu, G. Pompeo, R. Felici, Ordering and lyotropic behavior of a silicon-supported cationic and neutral lipid system studied by neutron reflectivity, Appl. Phys. Lett. 92 (2008) 193901. doi:10.1063/1.2917807.

[23] S. Bhattacharjee, DLS and zeta potential - What they are and what they are not?, J. Control. Release. 235 (2016) 337–351. doi:10.1016/j.jconrel.2016.06.017.

[24] J. Gallová, D. Uhríková, A. Islamov, A. Kuklin, P. Balgavý, Effect of cholesterol on the bilayer thickness in unilamellar extruded DLPC and DOPC liposomes: SANS contrast variation study., Gen. Physiol. Biophys. 23 (2004) 113–28.

[25] S. Labana, R. Pandey, S. Sharma, G.K. Khuller, Chemotherapeutic activity against murine tuberculosis of once weekly administered drugs (isoniazid and rifampicin) encapsulated in liposomes., Int. J. Antimicrob. Agents. 20 (2002) 301–4. doi:10.1016/S0924-8579(02)00175-9.

[26] N. Changsan, H.-K. Chan, F. Separovic, T. Srichana, Physicochemical characterization and stability of rifampicin liposome dry powder formulations for inhalation., J. Pharm. Sci. 98 (2009) 628–39. doi:10.1002/jps.21441.

[27] C. Rodrigues, P. Gameiro, M. Prieto, B. De Castro, Interaction of rifampicin and isoniazid with large unilamellar liposomes: Spectroscopic location studies, Biochim. Biophys. Acta - Gen. Subj. 1620 (2003) 151–159. doi:10.1016/S0304-4165(02)00528-7.

[28] A.V. Marques, P. Marengo Trindade, S. Marques, T. Brum, E. Harte, M.O. Rodrigues, M.G.M. D'Oca, P.A. da Silva, A.R. Pohlmann, I.D. Alves, V.R. de Lima, Isoniazid interaction with phosphatidylcholine-based membranes, J. Mol. Struct. 1051 (2013) 237–243. doi:10.1016/J.MOLSTRUC.2013.08.029.

[29] F. Domenici, F. Dell'Unto, D. Triggiani, C. Olmati, C. Castellano, F. Bordi, A. Tiezzi, A. Congiu, Vertical ordering sensitivity of solid supported DPPC membrane to alamethicin and the related loss of cell viability., Biochim. Biophys. Acta. 1850 (2015) 759–68. doi:10.1016/j.bbagen.2015.01.006.

[30] J. Li, X. Wang, T. Zhang, C. Wang, Z. Huang, X. Luo, Y. Deng, A review on phospholipids and their main applications in drug delivery systems, Asian J. Pharm. Sci. 10 (2015) 81–98. doi:10.1016/j.ajps.2014.09.004.

[31] P. Deol, G.K. Khuller, K. Joshi, Therapeutic efficacies of isoniazid and rifampin encapsulated in lung-specific stealth liposomes against Mycobacterium tuberculosis infection induced in mice., Antimicrob. Agents Chemother. 41 (1997) 1211–4.

Table 1. Particle size (nm), polydispersity index (PDI), Encapsulation Efficiency (EE %) and Drug Loading (DL %) of unloaded, single loaded liposomes and RIF/INH co-loaded liposomes (mean ± standard deviation).

Liposome content	**Z-Average (nm)**	**PDI**	**EE %**	**DL %**
Unloaded	350 ± 29	0.266 ± 0.030	-	-
RIF 3%	332 ± 33	0.283 ± 0.094	55.1 ± 6.1	1.7 ± 0.3
RIF 6%	347 ± 18	0.373 ± 0.115	55.3 ± 6.6	3.8 ± 0.1
RIF 12%	398 ± 15	0.440 ± 0.073	50.6 ± 7.1	5.9 ± 0.9
INH 15%	340 ± 25	0.124 ± 0.085	52.5 ± 6.2	7.8 ± 0.4
INH 30%	379 ± 51	0.262 ± 0.060	56.2 ± 2.8	14.9 ± 0.6
INH 60%	360 ± 8	0.200 ± 0.046	48.2 ± 0.9	22.4 ± 0.2
Co-loaded	361 ± 18	0.290 ± 0.032	RIF: 74.2 ± 6.4* INH: 71.3 ± 5.1$^{\#}$	RIF: 7.7 ± 0.7* INH: 9.2 ± 0.2$^{\#}$

$p^* < 0.05$ with respect to RIF 12% sample, $p^{\#} < 0.05$ with respect to INH.

Table 2. Best fit structural parameters obtained from the analysis of SANS curves of unloaded liposomes and for liposomes loaded with RIF and INH at different concentrations (core radius = r_c, lipid-drug shell span = t_s, lipid-drug SLD = ρ_s, water-drug shell span = t_w, water-drug SLD = ρ_0, layer number = N).

Fit parameters	**r_c (nm)***	**t_s (nm)***	**ρ_s (10^{-6} Å^{-2})**	**t_w (nm)***	**ρ_0 (10^{-6}Å^{-2})**	**N**	**Liposome Size (nm)**
Unloaded liposomes	170±3.4 [0.3]	5.0 [0.25]	2.38	1.8 [0.2]	6.42	6	418±7
RIF 3%	170±3.4 [0.3]	4.6 [0.3]	1.38	2.2 [0.2]	6.40	5	404±7
RIF 6%	180±3.6 [0.4]	4.0 [0.6]	0.17	2.7 [0.3]	6.30	3	390±7
RIF 12%	184±3.7 [0.4]	4.1 [0.5]	0.13	2.7 [0.4]	6.40	2-3	397±7
INH 15%	170±3.4 [0.2]	4.8 [0.3]	3.13	2.0 [0.6]	6.42	6	418±7
INH 30%	170±3.4 [0.2]	4.8 [0.3]	3.13	1.9 [0.6]	6.38	6	417±7
INH 60%	172±3.4 [0.2]	4.6 [0.3]	3.13	1.6 [0.6]	6.00	5	403±7

*The corresponding PDI values assuming a Gaussian distribution are reported in square brackets.

When not indicated, the standard deviations are ~ 2% of the fitting parameters values.

Table 3. Structural parameters of liposome loaded with both drugs obtained from the analysis of SANS curves (core radius = r_c, lipid-drug shell span = t_s, lipid-drug SLD = ρ_s, water-drug shell span = t_w, water-drug SLD = ρ_0, layer number = N).

Fit parameters	**INH 15% + RIF 12%**
r_c (nm)*	167±3.3 [0.3]
t_s (nm)*	4.8 [0.3]
ρ_s (10^{-6} Å^{-2})	3.06
t_w (nm)*	2.0 [0.6]
ρ_0 (10^{-6} Å^{-2})	6.40
N	4
Liposome Size (nm)	384 ± 7

*The corresponding PDI values assuming a Gaussian distribution are reported in square brackets.
When not indicated, the standard deviations are ~ 2% of the fitting parameters values.

Figure Captions

Figure 1. Multi-lamellar liposome representation showing the hypothesized localization of RIF and INH within its structure.

Figure 2. Multi-lamellar model of liposome showing the main parameters determined by SANS. The scattering length density SLD of the lipid layers ρ_s and the internal water layers ρ_0 depend on the material composition; the span of the layers is t_s, for the lipid phase and t_w for the inter-lamellar water phase.

Figure 3. *In vitro* release profiles from liposomes of a) RIF, b) INH.

Figure 4. SANS profiles of unloaded and RIF-loaded liposomes at various RIF concentrations. Best fits (solid lines) are superimposed to the experimental points (empty circles). The reduced χ^2 values associated to the best fits are 0.32 (black), 0.12 (red), 0.45 (blue), 0.25 (green).

Figure 5. SANS profiles of empty liposomes and INH-loaded liposomes at various INH concentrations. Best fits (solid lines) are superimposed to the experimental points (empty circles). The reduced χ^2 values associated to the best fits are 0.32 (black), 0.45 (red), 0.23 (green), 0.12 (blue).

Figure 6. SANS profile of liposomes loaded with both INH and RIF at different relative concentrations compared with the scattering curve of empty liposomes (in black). Best fits (solid lines) are superimposed to the experimental points (empty circles). The curves have been translated to better visualize the differences between the trends. The reduced χ^2 values associated to the best fits are 0.32 (black) 0.30 (dark cyan).

Graphical abstract